Comparison of two cationic polymeric flocculant architectures on the destabilization of negatively charged latex suspensions

Palomino, Daniel; Hunkeler, David; Stoll, Serge

How to cite

PALOMINO, Daniel, HUNKELER, David, STOLL, Serge. Comparison of two cationic polymeric flocculant architectures on the destabilization of negatively charged latex suspensions. In: Polymer, 2011, vol. 52, n° 4, p. 1019–1026. doi: 10.1016/j.polymer.2010.12.033

This publication URL: https://archive-ouverte.unige.ch/unige:18210
Publication DOI: 10.1016/j.polymer.2010.12.033

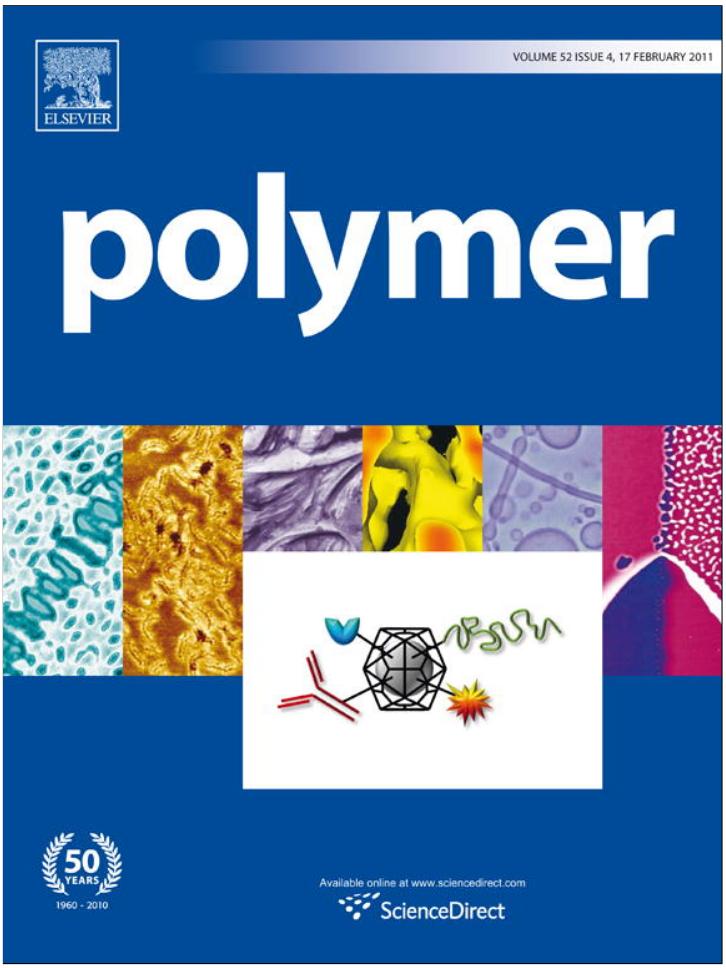

Polymer 52 (2011) 1019–1026

Contents lists available at ScienceDirect

Polymer

journal homepage: www.elsevier.com/locate/polymer

Comparison of two cationic polymeric flocculant architectures on the destabilization of negatively charged latex suspensions

Daniel Palomino [a], David Hunkeler [b], Serge Stoll [a,*]

[a] University of Geneva, F.-A. Forel Institute, Group of Environmental Physical Chemistry, 10 Route de Suisse, 1290 Versoix, Switzerland
[b] Aqua+TECH Specialties, chemin du Chalet-du-Bac 4, CH-1283 La Plaine, Switzerland

ARTICLE INFO

Article history:
Received 27 March 2009
Received in revised form
6 May 2010
Accepted 15 December 2010
Available online 22 December 2010

Keywords:
Linear and branched polyelectrolytes
Kinetics flocculation rate constants
Floc fractal dimensions

ABSTRACT

Flocculation studies between cationic polymers and oppositely charged colloidal particles are reported in which both flocculation kinetics and floc structures are systematically investigated. The flocculation rate constant, stability ratio and kinetics laws are experimentally determined using particle counting for two polymer architectures; a cationic linear polymer and a two-branched polymer. Comparisons are also made using NaCl at different ionic concentrations for the destabilization of the colloidal particles. Detailed measurements of electrophoretic mobility and kinetics rate constants on varying the polymer dosage are reported. Results suggest that the polymer architecture plays important roles on the polymer dosage for the rapid destabilization of the colloidal suspension. The branched polymer at optimal dosage exhibits the highest flocculation rate constant, whereas on the other hand, the linear polymer concentration range of flocculation is larger. In both cases, polymer flocculation is more efficient by a factor of 5–6 than charge screening effects due to the presence of salt. Analysis of the stability ratio indicates that tele-bridging flocculation and electrostatic forces dictate the stability of the charged latex particle suspension. It is shown that the fractal concepts which are valid for aggregation processes are also applicable here and branched polymers as well as linear polymers yield to the formation of compact flocs in comparison to those obtained with salt.

1. Introduction

In the aquatic systems, flocculation processes are playing essential roles in removing pollutants [1,2]. Trace metals and organic pollutants are mainly adsorbed at the surface of mineral particles like silicates, alumino-silicates or iron oxyhydroxides [3,4] owing to their high specific surface area, diffusivity and reactivity. In these systems algal and bacterial exudates composed of polysaccharide chains promote the flocculation of these mineral particles and the subsequent removal of pollutants. Flocculation is also used in numerous industrial processes such as water purification and wastewater treatment where flocculation is usually induced by positively charged synthetic polymers (polyelectrolytes) [5,6]. Considering wastewater treatment, the liquid phase needs to be rapidly separated with the highest efficiency from the solid one in order to obtain a clear filtrate, avoid to reject pollutants into natural aquatic systems, and maintain the maximum of pollutants in the minimum dry matter volume to minimize the waste quantity to treat, recycle or simply stock. Unfortunately, and for several reasons, polymeric flocculants are not always used in a rational way for optimal flocculation with regards to the natural fluctuations of the suspended material concentration, composition or, optimal dosage determination. Therefore, an improved understanding of the interaction mechanisms between cationic flocculants and colloidal particles is important for the rational use of polymeric flocculants. Furthermore, the synthesis of new polymer structures to accelerate coagulation rates beyond diffusion control and improve the efficiency of the flocculation processes by enlarging for example the polymer flocculation concentration range in which polymers are efficient is another important aspect [7,8].

From a fundamental point of view, there are two principal forces to consider in colloidal particle aggregation processes. The first concerns the long distance electrostatic repulsions between colloids which prevent coagulation while the second is related to the short distance van der Waals attractions which promote coagulation [9,10]. Simple electrolytes such as iron chloride ($FeCl_3$) or aluminium sulphate ($Al_2(SO_4)_3$), polysalts, including aluminium polychlorosulfates ($Al_xCl_y(SO_4)_z$), modify the nature of the electrostatic repulsions between particles by promoting electrostatic attractions [11–13]. As a result, the probability of forming permanent bonds between particles increases and screening effects, charge neutralization and charge

* Corresponding author. Tel.: +41 22 379 0333; fax: +41 22 379 0302.
E-mail address: serge.stoll@unige.ch (S. Stoll).

0032-3861/$ – see front matter © 2010 Elsevier Ltd. All rights reserved.
doi:10.1016/j.polymer.2010.12.033

inversion mechanisms are involved. The use of charged synthetic or biopolymers involves different mechanisms [7]. When the polymer radius of gyration is small in comparison to the particle size, aggregation is mainly promoted by local polymer adsorption and local inversion of the particle surface charges. Oppositely charged patches are then created which can interact with bare surfaces. Depending of the polymer concentration, complete surface charge neutralization can also be achieved at the colloid surface so that van der Waals forces, which are always attractive, can induce particle aggregation. However, if polymer dosage is not controlled, an excess of polymers will disperse the colloidal suspension by charge inversion or steric stabilization [14]. Polymer dosage is hence an important parameter for optimal destabilization of colloidal suspensions but also for economic reasons since excess of polymer represent extra costs. Three significant regimes have to be considered when i) polymer concentration is too low to induce rapid flocculation, ii) polymer concentration has an optimal value for rapid destabilization and iii) polymer concentration is too high and results in colloids restabilization [15]. It should be noted that, other than polymer dosage, there are several parameters to consider in order to achieve optimal flocculation conditions. They concern polymer geometry, polymer linear charge density and sign (oppositely charged polymer are usually used), and polymer intrinsic flexibility which are expected to control not only the aggregate structure but also the kinetics of flocculation. These parameters have to be considered for the rational synthesis of new flocculant structures. To show how little differences in some parameters can influence aggregation processes, Zhou and Franks [16] measured zeta potential and floc sizes of particle–polymer mixtures using Dynamic Light Scattering. They demonstrated that the flocculation mechanism of 90 nm silica particles, by addition of charged cationic polymers, was variable in accordance with polymer dosage, solid concentration, background electrolyte concentration and shear rate. Some parameters were correlated such as the increase of the polymer charge with the aggregate mass fractal dimension, reflecting the mechanisms involved. It was also observed that weakly charged polymers promote bridging whereas highly charged polymers induce electrostatic patch flocculation or full charge neutralization. Furthermore, it was shown that the polymer dosage influences both the aggregation mechanisms and the aggregate geometry. On the other hand, Yang [17] studied the flocculation of kaolin suspensions using small-angle laser light scattering. It was shown that the low molecular weight and highly charged polydiallyldimethylammonium chloride polymers induce aggregation by charge neutralization. The observed flocculation rate values were small and the resulting flocs compact. High molecular weight and relatively low charge density polymers were shown to promote bridging aggregation, high flocculation rates and less compact flocs. Rasteiro and Garcia [18] applied light diffraction spectroscopy to monitor the flocculation, deflocculation and reflocculation processes of cationic, linear and branched polyelectrolyte/precipitated calcium carbonate mixtures when different types of shear forces were applied. Floc resistance was correlated with floc structures, based on mass fractal dimension data. They also investigated the effect of the presence of inorganic salts on the polyelectrolyte performance and required flocculant dosage [19] showing that the presence of inorganic salts affects significantly the overall performance of the polyelectrolytes. Such studies also demonstrate that polymer molecular weight and charge are important parameters to consider in the understanding of flocculation mechanisms and floc geometry.

In this study, positively charged linear chains and positively charged branched polymers having two branches are used, and the influence of the polyelectrolyte microscale architecture on the kinetics of flocculation, polymer dosage, change of the electric properties of the colloidal particles, floc structures are addressed in an quantitative way. The polymers are evaluated on the destabilization of a solution containing well defined negatively charged particles. Optimal flocculation conditions and kinetics constants are determined by adjusting the polymer concentration. Stability ratio and collision efficiency parameters are calculated to get an insight into the parameters governing the flocculation processes. Floc structures are then examined to obtain the fractal dimension of the resulting structures. In all cases, flocculation rates, optimal polymer dosage and stability ratio are compared with salt induced particle destabilization (homocoagulation). Based on a detailed analysis of electrophoretic measurements and variations of the stability ratio, flocculation mechanisms are discussed, comparison is made with the salt situation and the validity of the DLVO theory to describe salt induced aggregation is verified.

2. Experimental

2.1. Flocculant composition and properties

Sodium chloride 99.5% from Acros Organics was used to adjust the solution electrolyte concentration and promote salt induced aggregation. Positively charged linear (AF BHMW) and the two-branched (AF B1^{++}) polyacrylamide polymers synthesized by Aqua + Tech Specialties S.A (Switzerland) [20,21] were used to induce the flocculation of well characterized and monodisperse latex particles. The polymer charge, molar mass and intrinsic viscosity are given in Table 1.

2.1.1. Materials

White crystals of acrylamide monomer *(AAM)* were supplied by Kemira water (formerly Cytec, Botlek, Netherlands) and used as received. Dimethylaminomethyl methacrylate (DMAEA) quaternized with methyl chloride was obtained from Ciba Specialty Chemicals (Bradford, England) as an aqueous solution (80%). For the polymerization in inverse-emulsion, the aqueous phase was emulsified in Exxsol D-100, a narrow cut of an isoparaffinic mixture without any VOCs (supplied by Exxon Chemical, Koln, Germany). Sorbitan monoisostearate (Montane 70) as well as polyethoxylated sorbitan monooleate (Montanox 80) purchased from Seppic (Paris, France) were also used as nonionic stabilizing agents. Type I reagent grade water with a resistance of 18.2 mΩ/cm was obtained through a series of deionization. 2,2′-azobis(2,4 dimethylvaleronitrile) (V-65, Wako Chemical, Germany) was used as received as oil soluble initiator. Certified ACS EDTA (ethylene diamine tetra-acetic acid, disodium salt dihydrate) (Fluka, Switzerland) was used as a chelating agent in the copolymerization with unpurified monomers. Adipic acid purchased from Riedel-de Haen (Seelze, Germany) was further used to prevent polymer hydrolysis. Rolfor TR/8 Cisalpina (Italy) was employed as wetting agent to invert the polymer-emulsions with excess water to yield a highly viscous dilute polymer solution.

2.1.2. Polymer synthesis

The polymerization reaction of acrylamide with dimethylaminoethyl acrylate quaternized methyl chloride, was performed in a 1-L stainless glass reactor cooled with a jacket and a water bath. The water-to-organic phase ratio was 2.7:1 by weight. The monomer concentration was nominally 40 wt% of the total mass of emulsion and the emulsifier blend was dissolved in the organic phase at

Table 1
Polymer properties (cationic flocculants). η represents the intrinsic viscosity, R_h the hydrodynamic radius and ζ the zeta potential.

Name	Charge [Wt %]	Number of branches	η [mL/g]	Molar mass [10^6 g/mol]	R_h [nm]	ζ [mV]
AF BHMW	80	0	1720	7.2	311 ± 11	+72 ± 3
AF B1^{++}	80	2	2636	12	252 ± 21	+78 ± 3

a concentration of 2.3 wt% of the total reaction mass. The HLB value was approximately 5.8. The chemical initiator 2,2′-azobis(2,4-dimethyvaleronitrile) (V-65, Wako Chemicals. Neuss, Germany) dissolved into xylene was added into the reactor at 40 °C. The reaction time was 6 h and following an isothermal period of 1–2 h the reaction was allowed to exotherm to a temperature between 70 and 80 °C.

2.1.3. Inversion and viscometric characterization of the inverse-emulsion

The inversion of polymerized inverse-emulsions was carried out as follows. In a large and baffled beaker (l-L capacity), 500 g of deionized water was stirred at 400 rpm (Rushton type of impeller). A precalculated amount of emulsion (containing the inverting surfactant) was added to yield 0.1 wt% active weight of polymer in solution was added within a short time (less than 1 s) directly to the center of the vortex. The agitation speed was further increased to 600 rpm and maintained for an additional 5 min. A rapid increase in solution viscosity and the absence of agglomerates in the aqueous phase usually indicated a good inversion. The resulting polymer diluted solution was then characterized by viscosity measurements. The polymer viscosity was measured with a model L VDVII + viscometer (Brookfield, Stoughton, MA, USA) at 50 rpm and room temperature [22].

2.2. Latex particle properties

Monodisperse spheres of latex polystyrene from IDC (Interfacials Dynamics Corporation) were used. Their mean diameter was determined by TEM and found equal to 0.99 ± 0.03 μm. The spheres were provided in an aqueous suspension containing 81 g/L of latex particles. The particle number, per milliliter of solution, equalled to 1.5×10^{11} and the specific surface area to 5.7×10^4 [cm^2/g]. The latex particles exhibit negatively charged surfaces due to the presence of sulphate groups (7.6×10^5 per particle) and the charge density has a constant value equal to 3.9 [μC/cm^2] for pH values above 4. The charge content, equal to 2.3 [μEq/g], was determined using conductimetric titrations. The Zeta potential of the latex particles was measured with a Malvern Zetasizer Nano and found equal to -100 ± 3 mV for a NaCl concentration equal to $1.5 \cdot 10^{-4}$ M.

2.3. Size distribution determination and zeta potential measurements

A Coulter® Counter Multisizer II™ was used to measure the decay of the number of colloidal monomers (free particles) with time. This device determines through 256 channels the equivalent size (from 1 to 30 μm) and number of particles or aggregates passing through an aperture orifice of 50 μm. Each measurement is performed during 30 s corresponding to 287 μl of solution. Isoton™ IIA was used as a support electrolyte. It was pre-filtered with a 0.22 μm Millipore® ISOPORE™ GTTP filter to reduce the background noise. It should be noted here that the diameter given by Coulter® Counter corresponds to the diameter of the sphere equivalent to the aggregate as if all the latex monomers were collapsed in one compact volume. In order to determine experimental kinetics aggregation rates K_S, the decrease with time of the free latex particles number has been followed in the 1 μm channel in order to take into consideration only non aggregated particles (free monomers).

The Malvern Zetasizer Nano instrument was used to measure the zeta potential of the latex particles in solution as a function of flocculation time and polymer concentration. Each sample was measured 5 times with 15 sub-runs for each measure. Between runs a pause of 10 s was imposed to allow the system to relax and stabilize before the next measurement.

2.4. Determination of the aggregate fractal dimension D_f

Mandelbrot [23] introduced fractal dimension concepts to various objects such as colloidal aggregates to quantitatively describe their structural properties. To gain insight into the aggregate structures, by considering mass distribution in space, flocs were magnified 40 times with a Laborlux S microscope from Leitz. Images were taken with a Nikon D90 then treated with the SigmaScan Pro 4 software to enhance the contrast between the background and the aggregates. The total number of aggregates, relative masses (in term of total number of pixels) and aggregate dimensions (here the major axis lengths) were calculated to determine D_f according to the scaling law relationship [24]:

$$m \sim l^{D_f} \tag{1}$$

where m represents the aggregate mass (number of pixels) and l the aggregate major axis length in reduced coordinates. D_f was calculated by considering a log/log plot of m versus l. In order to validate this method we applied this procedure to solid spheres and lines and D_f values equal to 2.00 ± 0.01 and 1.05 ± 0.03 respectively were found in good agreement with the theoretical expected values [24].

3. Results and discussions

3.1. Aggregation in presence of salt

The influence of the concentration of simple electrolyte on the aggregation kinetics of latex suspensions was investigated first. Salt is expected to screen the electrostatic repulsive forces between latex particles. Increasing the salt concentration C_i is thus expected to result in an increase of the aggregation rate constant. Suspension containing 0.5 g/L suspensions of latex particles have been destabilized at 25 °C by adjusting the final salt concentrations to 0.15, 0.18, 0.2, 0.25, 0.5 and 1 M in orthokinetic conditions at a mixing speed of 100 ± 2 RPM.

From the monomer number evolution with time the aggregation rate constants K_S were calculated and compared to 1st and 2nd order kinetic laws. Aggregation rate constants K_S were found to follow a 2nd order process according to:

$$\frac{dN_1}{dt} = -K_S|N_1|^2 \tag{2}$$

A linear proportionality between time and the inverse of the number of free particles N_1 was found (Fig. 1).

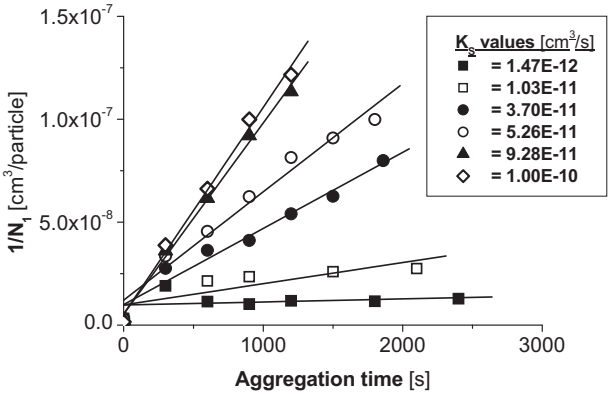

Fig. 1. Experimental kinetic aggregation rates K_S [cm^3/s] values obtained from the evolution of the inverse number of free particles versus time during the destabilization of 0.5 g/L solutions of negatively charged latex particles using different NaCl salt concentrations : ■ = 0.15, □ = 0.18, ● = 0.2, ○ = 0.25, ▲ = 0.5, ◇ = 1M.

K_S was directly obtained from the slope value for each salt concentration and was found to increase continuously with increasing C_i. The initial number of particles at t_0 was determined by the Coulter Counter in order to get more accurate linear regressions [25]. To get an insight into the aggregation rate constant variation with salt concentration, K_S values are summarized in Fig. 2. A rapid increase of K_S is observed at $C_i = 0.15$M followed by a plateau for salt concentrations greater than 0.5M.

Using the DLVO theory [9,10], the experimental K_S evolution with C_i was compared with theoretical calculations of the total interaction potentials between two latex particles (Fig. 3). The total interaction potential $V_T(H)$ was expressed as the sum of the van der Waals attractive forces $V_{vdW}(H)$ and electrostatic repulsive forces $V_{el}(H)$. The van-der-Waals-Hamaker and the Linear Superposition Approximation [25,26] were used to evaluate $V_{vdW}(H)$ and $V_{el}(H)$:

$$V_{vdW}(H) = -\frac{A_{1,3,1}}{6}\cdot\left\{\frac{2a^2}{H(H+4a)}+\frac{2a^2}{(H+2a)^2}+\ln\left(\frac{H(H+4a)}{(H+2a)^2}\right)\right\} \quad (3)$$

$$V_{el}(H) = 2\pi\varepsilon_0\varepsilon_r a\Psi_0^2 e^{-\kappa H} \quad (4)$$

where $A_{1,3,1}$ represents the Hamaker constant which corresponds to 1.40×10^{-20} [J] and represents an average value for latex particles [27–29], a the radius of the latex particle (0.5 μm) and H the distance between the two particle surfaces. ε_0 and ε_r are respectively the vacuum permittivity and the water relative permittivity whereas Ψ_0 represents the latex surface potential which was calculated for each ionic strength [15]. Finally, the Debye-Hückel parameter [15,28] was calculated according to :

$$\kappa = \sqrt{\frac{2n_0e_0^2}{\varepsilon_r\varepsilon_0k_BT}} \quad (5)$$

By comparing Figs. 2 and 3, good agreement is found between the experimental values and the theoretical predictions. Fig. 3 shows that within the range 0.25–1M NaCl the interaction curves are fully attractive; particles can aggregate rapidly and this situation corresponds to the maximum aggregation rate plateau value observed in Fig. 2 when NaCl concentration $C_i \geq 0.4$. When $C_i < 0.25$M, due to the presence of an energetic barrier, particles repel significantly hence reducing the aggregation rate. In such

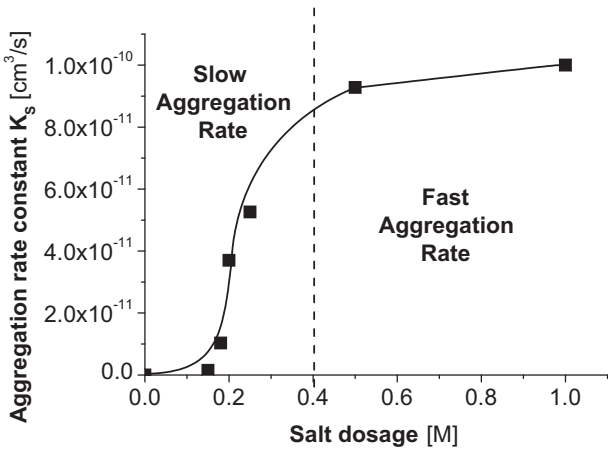

Fig. 2. Evolution of K_S with NaCl salt dosage concentration. The vertical dotted line corresponds to the salt concentration at which the interaction potential between the surfaces of two latex particles results in fast aggregation rate.

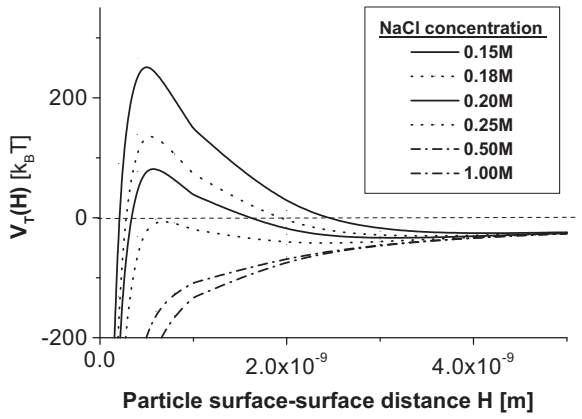

Fig. 3. DLVO interaction potentials between two latex particles as function of : i) the distance H between their surfaces by considering the contribution of the van der Waals attractive forces and the repulsive electrostatic forces and ii) by adjusting the salt concentration C_i. It should be noted that the repulsive energetic barrier disappears when $C_i \geq 0.25$M.

cases, the effect of colloid interactions is often expressed as a collision efficiency factor α (with $0 \leq \alpha \leq 1$). A collision efficiency of unity implies that every collision leads to permanent attachment. Repulsion forces reduce the collision efficiency such that practically no aggregation occurs. Because of the key role played by this parameter, the sticking probability α was determined by considering the ratio between the rate constant determined in the fast aggregation regime at high salt concentration, and assuming a value $\alpha = 1$ for the highest aggregation rate constant value obtained experimentally [14]. For example, the sticking probability was assumed to be equal to 0.10 at 0.18M NaCl indicating that 10% of the collisions between elementary particles result in the formation of a permanent bond.

The reciprocal value of α, $w = 1/\alpha$, known as the stability ratio w was calculated and presented in Fig. 4 as a function of the salt concentration. Fig. 4 shows that log w decreases linearly when log [NaCl] increases. When [NaCl] > 0.2M, log w becomes constant and equal to 1. This value of [NaCl] corresponds to the Critical Coagulation Concentration (CCC = 0.2M). For [NaCl] < CCC, the energy barrier disappears and particle aggregation can occur at a maximum

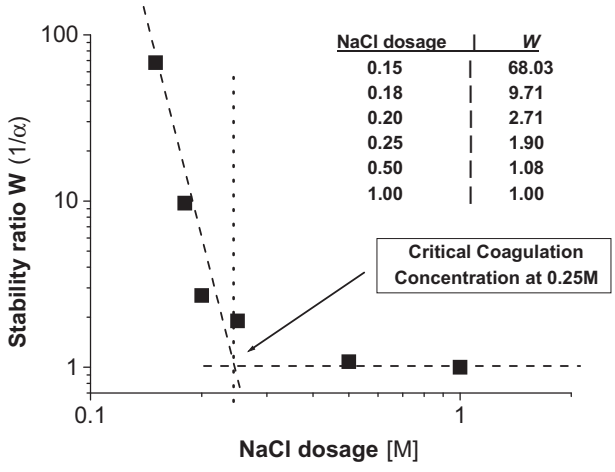

Fig. 4. The Critical Coagulation Concentration (CCC) is determined by plotting the inverse of the sticking probability (stability ratio w) as a function of the salt concentration. The α (sticking probability) values for the different NaCl concentrations are presented in the insert. The CCC value corresponds to a salt concentration equal to 0.25M.

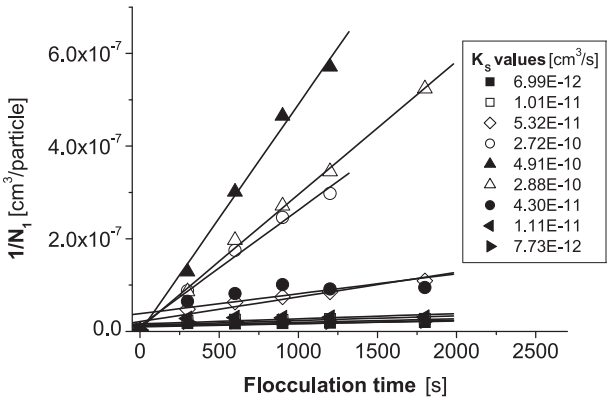

Fig. 5. Variation of the inverse of the number of free latex particles as a function of the flocculation time. Experimental K_S values in the inset are obtained from the different slopes and for the destabilization of 0.5 g/L solutions of latex particles at different linear polymer AF BHMW concentrations: ■ = 3, □ = 3.5, ◇ = 4, ○ = 4.5, ▲ = 4.75, Δ = 5, ● = 5.25, ◄ = 5.5, ► = $6 \cdot 10^{-4}$ g/L.

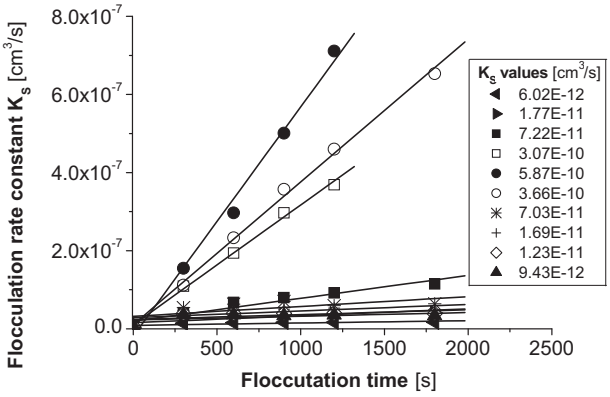

Fig. 7. Experimental K_S values obtained during the destabilization of 1 g/L solutions of latex particles at different branched polymer AF B1^{++} concentrations: ◄ = 8, ► = 10, ■ = 11, □ = 12, ● = 12.5, ○ = 13, * = 13.5, + = 14, ◇ = 15, ▲ = $16 \cdot 10^{-4}$ g/L.

rate, determined by the transport rate and the collision frequency between latex particles.

3.2. Flocculation in presence of linear cationic polymer chains

The destabilization of the latex suspension is now investigated by using oppositely charged linear polymers (AF BHMW). 1 g/L suspensions of latex particles have been considered at 25 °C by adjusting the final AF BHMW concentrations to 3, 3.5, 4, 4.5, 4.75, 5, 5.25, 5.5, 6, 7 [10^{-4} g/L] and at a constant mixing speed equal to 100 ± 2 RPM. The kinetic law is also found to follow a 2nd order process, since a linear proportionality between time and the inverse of the number of free particles N_1 is only obtained in such conditions (Fig. 5).

K_S values are directly obtained from the slope values in Fig. 5. As shown in Fig. 6, representing the K_s variations as a function of the polymer dosage, and in contrast to the salt effect which promotes aggregation until a maximum plateau value, the increase of polymer concentration is first promoting the flocculation of latex suspensions until a maximum value which represents the optimal flocculant dosage. After this point, the increase of polymer concentration stabilizes the latex suspension. It is important to note here that the highest K_S value is about 5 times higher than the one obtained previously using salt. The adsorbed polymer here significantly decreases the suspension stability and accelerates the aggregation rate beyond diffusion control. One complementary information can also be extracted from Fig. 6: the polymer effective flocculation dosage window. The width of the polymer dosage window gives information about the polymer efficiency concentration domain. The larger is the window, the more efficient will be the flocculant in different situations resulting for example from initial particle concentration variations. Another important parameter is the zeta potential of the free latex particles which is also presented in Fig. 6. The zeta potential variations show that the free latex particles are still negatively charged within the range of the effective window of flocculation. This parameter gives important information about the polymer flocculation mechanism which is discussed more in detail in Section 3.4.

3.3. Flocculation in presence of branched cationic polymer chains

The behaviour of the latex suspension is then investigated by using the oppositely charged two-branched polymers (AF B1^{++}). In order to compare from a kinetic point of view the linear and branched polymer behaviour we used strictly the same procedure and parameters for both experiments, varying only the polymer geometry. The calculated K_S values as a function of the AF B1^{++} polymer concentration are presented in Fig. 7.

The highest K_S value obtained at optimal polymer dosage is equal to 5.87×10^{-10} [cm^3/s]. Such a value is about 6 times higher than the maximum value obtained with the salt experiment and significantly higher than the highest K_S value obtained with the linear polymer at optimal dosage. As for AF BHMW, Fig. 8 shows

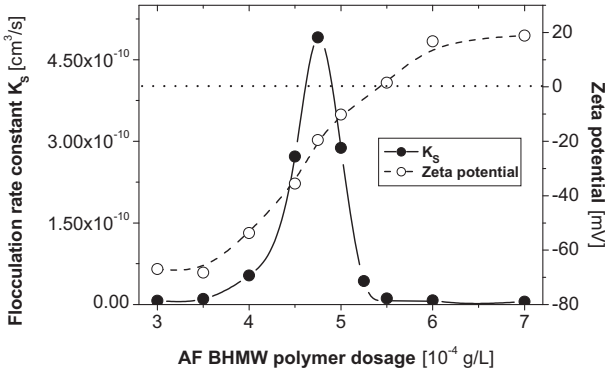

Fig. 6. K_S and zeta potential evolutions as a function of the concentration of AF BHMW polymer. The K_S maximum value is obtained at $4.75 \cdot 10^{-4}$ g/L of linear polymer and for a zeta potential value equal to −19 mV. The effective flocculation window corresponds to a polymer concentration range from 3.5 to 5.5 [10^{-4} g/L] and zeta potential range from −60 to −10 mV.

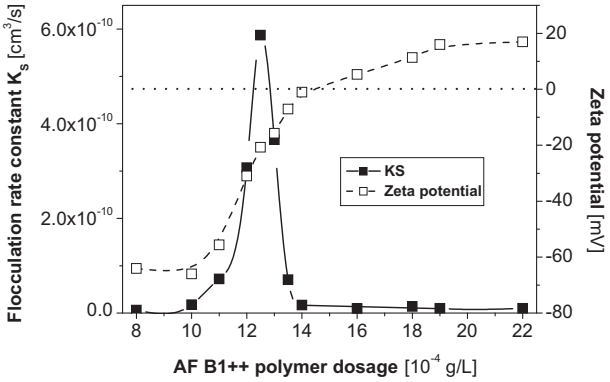

Fig. 8. K_S and zeta potential evolution as a function of AF B1^{++} polymer concentrations. The K_S maximum value is obtained at $12.5 \cdot 10^{-4}$ g/L of branched polymer and for a zeta potential value of −21 mV. The effective flocculation window corresponds to a polymer concentration range from 10.5 to 13.5 [10^{-4} g/L] and zeta potential range from −50 to −10 mV.

that using AF B1^{++} the free latex particles are still negatively charged within the range of the effective window of flocculation.

For comparison, the corresponding stability ratio evolution of the two polymers with dosage is presented in Fig. 9. Two main differences between the linear and branched polymers are found: i) branched polymers destabilize the latex suspensions significantly faster than the linear polymers ii) the width of the linear polymer dosage window is substantially larger than the branched one. Such observations reveal a better efficiency at the optimal dosage for the AF B1^{++} despite the fact that more important quantities are needed. The Critical Flocculation Concentration* (CFC*) and CFC** [30,31] are also calculated and presented in Fig. 9. The evolution of w can be described into three different regimes: i) one region where flocculation is increased (decrease of the stability ratio w) by increasing the polymer dosage. The maximum value obtained in this region is represented by the CFC*, ii) a second region where the stability ratio w has its maximum value and the polymer its maximum efficiency, iii) a third region where w increases again indicating the stabilization of the colloid suspension.

3.4. Flocculation mechanisms

To get an insight into the flocculation mechanisms, IDC latex spheres, linear and branched polymer hydrodynamic radius R_h were measured by DLS with a Malvern Zetasizer Nano ZS. The results below show that polymer R_h, respectively 311 ± 11 nm for linear polymers and 252 ± 20 nm for two-branched polymers, are slightly lower than the IDC particle R_h which is equal to 508 ± 37 nm. Experiments clearly demonstrate that the latex particle zeta potential is increasing with the polymer dosage from −100 mV up to charge reversal and stabilization at +20 mV. Here polymer adsorption leads to the characteristic charge reversal (or overcharging) of the latex particles after one isoelectric point (IEP). When adding polymer at the optimal flocculation dosage, the zeta potential is found close to −20 mV for both linear and branched polymer denoting that, in the two cases, the main flocculation mechanism is not related to a charge neutralization process. Also owing to the hydrodynamic radius and molar masses of the two polymers, the patch neutralization process is not expected, at optimal dosage, to play an important role. These findings suggest that "tele-bridging" flocculation and electrostatic forces dictate the stability of our oppositely charged latex particle suspension. The stability ratio w versus the polymer dose which is shown in Fig. 9 reveals the important finding of this paper. One observes the characteristic "U" shaped plots with the minimum situated at optimal dosage and before the IEP. After the IEP, by

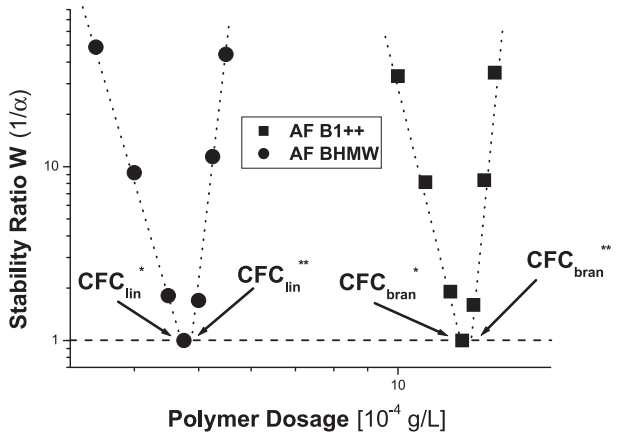

Fig. 9. Log–log plot of the stability ratio w versus the AF BHMW and AF B1^{++} polymer concentrations. The Critical Flocculation Concentrations$^{*/**}$ (CFC* and CFC**) were determined for both polymers respectively CFC$_{lin}^{*/**}$ for AF BHMW and CFC$_{bran}^{*/**}$ for AF B1^{++}.

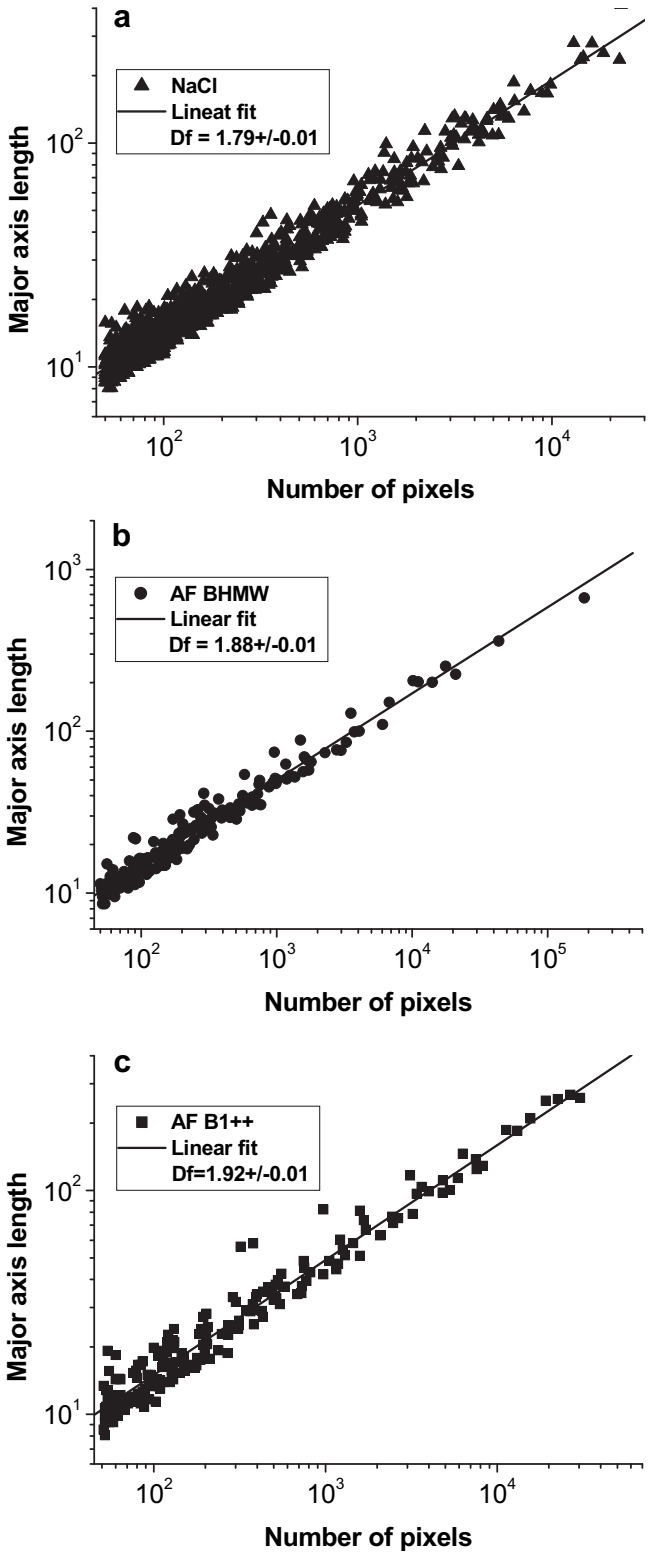

Fig. 10. Log–log plot of the major axis length as a function of number of pixels for the aggregates obtained by destabilization of latex suspensions after 2400 s and at optimal dosage of: (a) NaCl, (b) linear polymer, (c) branched polymer. Average D_f values obtained by analyzing 10 pictures of each solution, and by considering three decades in number of pixels, correspond to 1.80 ± 0.02 with NaCl, 1.88 ± 0.04 with the linear polymer and 1.91 ± 0.03 with the branched polymer.

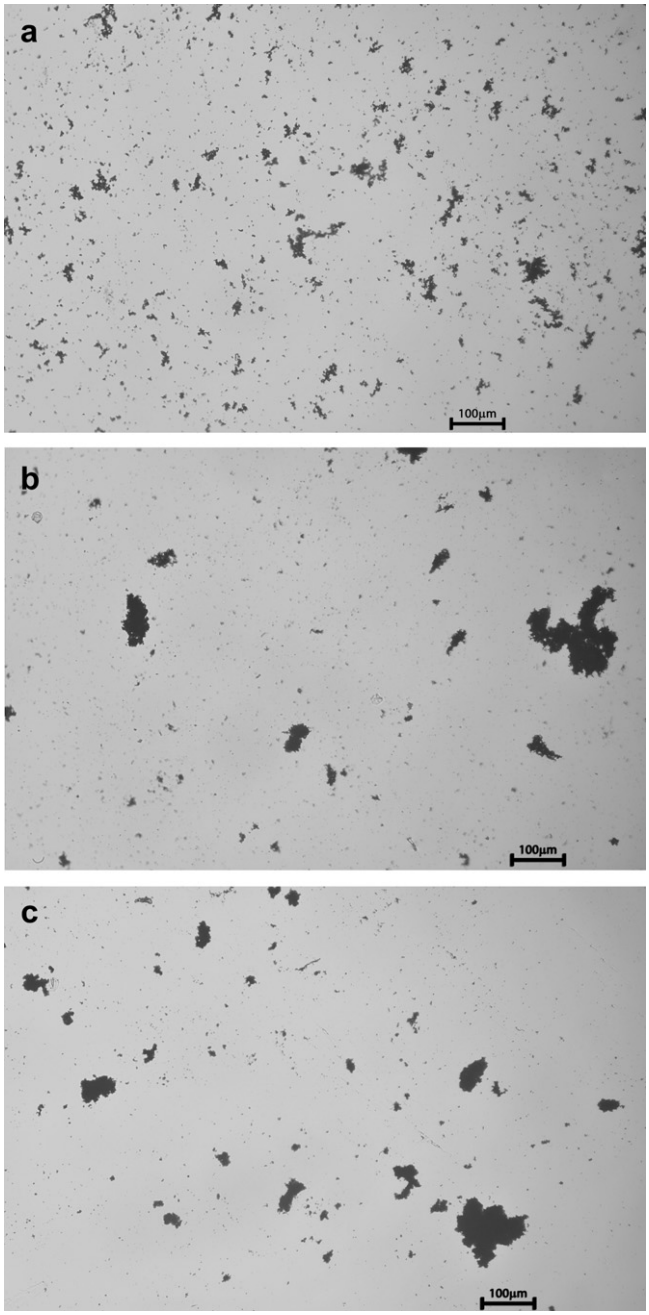

Fig. 11. Aggregate and floc pictures obtained by destabilization of latex suspensions at optimal dosage using : (a) NaCl, (b) linear polymer, (c) branched polymer. Large structures are observed for both polymers in agreement with the high kinetics aggregation rates. Aggregates obtained with salt are smaller and exhibit open structures.

increasing the polymer dose, a steric stabilization, due to bound polymer layers at the latex particles is achieved hence preventing them from coagulation via attractive van der Waals forces. One also observes in Fig. 9 that the stability ratio is rapidly increasing after the CFC** (asymmetric "U" shaped). Indeed, after the CFC**, steric and electrostatic stabilization of the polymer is rapidly achieved owing to the relative large dimensions of the two polymers in comparison to the latex particle sizes.

3.5. Determination of the floc structures

In order to evaluate the fractal character and calculate the floc fractal dimensions in presence of salt, linear and branched polymers, flocs were collected after 2400 s at optimal salt and polymer dosage (respectively: 0.5M, $4.75 \cdot 10^{-4}$ g/L and $1.25 \cdot 10^{-3}$ g/L). For each situation, 10 samples representing at least 1000 aggregates were analysed. In Fig. 10 is presented on log–log plots the variation of the flocs major axis lengths as a function of their masses (number of pixels). Pictures corresponding to the resulting flocs are given in Fig. 11 for the salt, linear and branched polymers. The fractal dimension D_f (1.80 ± 0.02) of aggregates induced by NaCl charge screening is in good agreement with the common values found for the cluster–cluster aggregation model [32,33] for the diffusion limited aggregation process (DLCA) which results in the formation of open structures.

Flocs induced by linear and branched polymers exhibit significant higher D_f values, respectively 1.88 ± 0.04 and 1.91 ± 0.03, denoting that theses flocs are more compact and larger in good agreement with the respective kinetics rate constants. There is a noteworthy difference between flocs induced by the presence of linear polymers and those by branched polymers which are more dense.

4. Conclusions

A Coulter Counter was used to investigate in a systematic way the floc formation between negatively charged particles and oppositely charged polymeric flocculants. Kinetics aspects as well as structural parameters (fractal dimensions) with special focus on the effects of polymer dosage were investigated. The role of polymer dosage on the flocculation rate constants, stability ratio w variations and the determination of the CCC were also investigated and a systematic comparison was made with salt induced particles aggregation for a better estimation of polymer efficiency and optimal dosage concentration range.

Our study points out the differences between the flocculation and the salt induced destabilization mechanisms. At optimal polymer dosage, the flocculation rate constants are significantly larger than the aggregation rate constant obtained with salt i.e. when charge screening has reached its optimal effect. The structure of the polymer is shown to play a significant role on the kinetics of flocculation, floc characteristics, and the range of concentration over which flocculation occurs. Optimal polymer dosage concentration is higher for the branched polymer which exhibits a greater flocculation rate constant, whereas the linear polymer is shown to have a larger concentration domain of use.

Overall, our findings suggest that bridging flocculation and electrostatic forces dictate here the stability of the charged latex particle suspension, in comparison to charge neutralization and patch formation flocculation mechanisms. Another interesting result of this study is the fact that the analysis of the resulting structures clearly demonstrates the fractal character of the flocs and exhibits a significant difference between the two polymers denoting the importance of the polymer architecture not only in the kinetics rate constant and concentration range, but also in the fractal floc structure which is expected to control important floc properties such as floc settling velocity and cohesion. Mixtures of polymers and salt will be investigated in a future paper to gain insight into the effect of charge screening on the polymeric flocculant efficiency.

Acknowledgments

The authors are grateful to E. Pefferkorn, J. Buffle, J.L. Loizeau, S. Ulrich, M. Seijo, F. Carnal for useful discussions and comments. The authors also acknowledge the Aqua + Tech Specialties SA (La Plaine, Geneva, Switzerland) for supplying the flocculant samples.

References

[1] Buffle J, Vitre RRD. Chemical and biological regulation of aquatic systems. CRC Press; 1994.
[2] Santschi P. Particle flux and trace metal residence time in natural waters. Limnol Oceanogr 1984;29:1100–8.
[3] Buffle J, Wilkinson K, Stoll S, Filella M, Zhang J. A generalized description of aquatic colloidal interactions: the three-colloidal component approach. Environ Sci Technol 1998;32:2887–99.
[4] Wilkinson KJ, Balnois E, Leppard GG, Buffle J. Characteristic features of the major components of freshwater colloidal organic matter revealed by transmission electron and atomic force microscopy. Colloids and Surfaces A: Physicochemical and Engineering Aspects 1999;155:287–310.
[5] Schwoyer W, editor. Polyelectrolytes for water and wastewater treatment; 1981.
[6] Gregory J. Particles in water properties and processes; 2005.
[7] Stoll S, Buffle J. Computer simulation of bridging flocculation processes: the role of colloid to polymer concentration ratio on aggregation kinetics. Journal of Colloid and Interface Science 1996;180:548–63.
[8] Agarwal M, Srinivasan R, Mishra A. Synthesis of *Plantago Psyllium* mucilage grafted polyacrylamide and its flocculation efficiency in tannery and domestic wastewater. Journal of Polymer Research 2002;9:69–73.
[9] Verwey E, Overbeek J. Theory of the stability of lyophobic colloids. Dover Publications; 1948.
[10] Deryagin B, Landau L. Theory of the stability of strongly charged lyophobic sols and of the adhesion of strongly charged particles in solutions of electrolytes. Acta Physicochim. URSS 1941;14:633–62.
[11] Van Benschoten JE, Edzwald JK. Chemical aspects of coagulation using aluminum salts-I. Hydrolytic reactions of alum and polyaluminum chloride. Water Research 1990;24:1519–26.
[12] Van Benschoten JE, Edzwald JK. Chemical aspects of coagulation using aluminum salts-II. coagulation of fulvic acid using alum and polyaluminum chloride. Water Research 1990;24:1527–35.
[13] Duan J, Gregory J. Coagulation by hydrolysing metal salts. Advances in Colloid and Interface Science 2003;100–102:475–502.
[14] Ferretti R, Stoll S, Zhang J, Buffle J. Flocculation of hematite particles by a comparatively large rigid polysaccharide: schizophyllan. Journal of Colloid and Interface Science 2003;266:328–38.
[15] Elimelech M, Williams R, Jia X, Gregory J. Particle deposition and aggregation: measurement, modeling and simulation. Butterworth-Heinemann; 1997.
[16] Zhou Y, Franks G. Flocculation mechanism induced by cationic polymers investigated by light scattering. Langmuir 2006;22:6775–86.
[17] Yu J, Wang D, Ge X, Yan M, Yang M. Flocculation of kaolin particles by two typical polyelectrolytes: a comparative study on the kinetics and floc structures. Colloids Surf., A 2006;290:288–94.
[18] Rasteiro M, Garcia F, Ferreira P, Blanco A, Negro C, Antunes E. Evaluation of flocs resistance and reflocculation capacity using the LDS technique. Powder Technology 2008;183:231–8.
[19] Antunes E, Garcia FAP, Ferreira P, Blanco A, Negro C, Rasteiro MG. Effect of water cationic content on flocculation, flocs resistance and reflocculation capacity of PCC induced by polyelectrolytes. Industrial & Engineering Chemistry Research 2008;47:6006–13.
[20] Barajas J, Hunkeler D, Wandrey C. Polyacrylamide copolymeric flocculants with homogeneous branching: hetereophase synthesis and characterization. Polym News 2004;29:239–46.
[21] Hunkeler D, Wandrey C. Polyelectrolytes: research, development, and applications. International Journal for Chemistry 2001;55:223–7. Chimia.
[22] Stoll S, Wandrey C, Hünkeler D. Rational Formulation of Water Based Flocculants: Interactions, local Nanostructure and Dimensions. in Preparation. (sans date).
[23] Mandelbrot B. The fractal geometry of nature. San Francisco: W.H. Freeman; 1982.
[24] Senesi N, Wilkinson KJ. Biophysical chemistry of fractal structures and processes in environmental systems. Wiley; 2008.
[25] Lopez J. Electrostatic heteroaggregation process arising in two-component colloidal dispersion; 1996.
[26] Plaza RC, Quirantes A, Delgado AV. Stability of dispersions of colloidal hematite/yttrium oxide core-shell particles. Journal of Colloid and Interface Science 2002;252:102–8.
[27] Rubio-Hernandez FJ. On the Hamaker function of polystyrene model colloids. Colloids and Surfaces A: Physicochemical and Engineering Aspects 1994;88:141–5.
[28] Hunter RJ. Foundations of colloid science. 2nd ed. USA: Oxford University Press; 2001.
[29] Puertas AM, de las Nieves FJ. Colloidal stability of polymer colloids with variable surface charge. Journal of Colloid and Interface Science 1999;216:221–9.
[30] Liang W, Bognolo G, Tadros TF. Stability of dispersions in the presence of graft copolymer. 1. Adsorption of graft copolymers on latex dispersions and the stability and rheology of the resulting dispersions. Langmuir 1995;11:2899–904.
[31] Sharma A, Tan SN, Walz JY. Measurement of colloidal stability in solutions of simple, nonadsorbing polyelectrolytes. Journal of Colloid and Interface Science 1997;190:392–407.
[32] Weitz DA, Oliveria M. Fractal structures formed by kinetic aggregation of aqueous gold colloids. Phys. Rev. Lett. 1984;52:1433.
[33] Waite TD. Measurement and implications of floc structure in water and wastewater treatment. Colloids and Surfaces A: Physicochemical and Engineering Aspects 1999;151:27–41.